# A novel route towards high quality fullerene-pillared graphene

Spyrou, Konstantinos; Kang, Longtian; Diamanti, Eumorfia K.; Gengler, Regis Y.; Gournis, Dimitrios; Prato, Maurizio; Rudolf, Petra

*Published in:*
Carbon

*DOI:*
10.1016/j.carbon.2013.05.010



*Publication date:*
2013

CARBON 61 (2013) 313–320

Available at www.sciencedirect.com

SciVerse ScienceDirect

journal homepage: www.elsevier.com/locate/carbon

# A novel route towards high quality fullerene-pillared graphene

Konstantinos Spyrou [a,*], Longtian Kang [a], Evmorfia K. Diamanti [b], Regis Y. Gengler [a], Dimitrios Gournis [b], Maurizio Prato [c], Petra Rudolf [a]

[a] Zernike Institute for Advanced Materials, University of Groningen, Nijenborgh 4, NL-9747 AG Groningen, The Netherlands
[b] Department of Materials Science and Engineering, University of Ioannina, GR-45110 Ioannina, Greece
[c] Dipartimento di Scienze Chimiche e Farmaceutiche, Università degli Studi di Trieste, Piazzale Europa 1, I-34127 Trieste, Italy

ARTICLE INFO

*Article history:*
Received 6 February 2013
Accepted 4 May 2013
Available online 14 May 2013

ABSTRACT

A new approach for the synthesis of graphite intercalation compounds (GICs), by the help of co-intercalant molecules, has been observed. In the present work, we demonstrate the successful incorporation of fullerene ($C_{60}$) molecules between the graphene sheets aided by the preceding intercalation of nitric acid. The presence of intercalated $C_{60}$ between the graphene sheets is deduced from X-ray diffraction patterns, while Raman and X-ray photoelectron spectroscopy (XPS), verify that the quality of the graphene layers is not compromised by the intercalation. A quantification of the interaction yield was derived from thermogravimetric analysis and XPS studies, giving that fullerene molecules intercalated in the pillared structure amount to about 25 wt%. The present method opens new perspectives for the intercalation of various guest molecules in graphite also because graphite nitrate allows for functionalization processes following the very well established carbon chemistry.



## 1. Introduction

Carbon is the element with the highest number of known allotropes. The three best-known ones are amorphous carbon, graphite, and diamond. In the past 30 years, new forms have been synthesized, including carbon nanotubes, graphene, and fullerenes, all of which have had a significant scientific and technological impact due to their unique properties, such as high surface area, good thermal and chemical stability, low mass, chemical inertness and unusual electronic properties [1–4]. These materials have been extensively used as electrochemical storage capacitors, catalytic substrates, sorbents for separation processes, gas sensors, gas storage materials at high temperatures (*e.g.*, for hydrogen, $CO_2$, methane) [5–8]. On the other hand, the big challenge in the field of nanoporous materials is the creation of mesoporous structures with controlled porosity and very high/tunable surface area [9], since both of which are decisive factors for applications in catalysis and energy storage [10]. Graphene, the one atom thick layer of $sp^2$ hybridized carbon atoms, with its very high surface area, (2500 $m^2/g$), is an excellent candidate for the development of novel hybrid nanoporous materials since it is also easily modifiable (chemically) and presents outstanding mechanical and thermal stability [11]. To create a porous material, one has to prevent graphene layers from assembling to form graphite driven by van der Waals interaction between the aromatic π-systems and a way to do this is to insert robust organic/inorganic species as columns/pillars in between them, using the so-called 'pillaring method' [12]. This method has been successfully employed with other layered materials like clays [13], and layered double hydroxides [14]. By choosing the right guest molecules which are stable enough to keep the graphene layers separate, the appropriate distance for achieving a high surface area can be obtained. To

* *Corresponding author:* Fax: +30 26510 07074.
E-mail addresses: K.Spyrou@rug.nl, kos_spy@hotmail.com (K. Spyrou).
0008-6223/$ - see front matter 
http://dx.doi.org/10.1016/j.carbon.2013.05.010

succeed in making such a pillared structure starting from graphite, two basic steps must be accomplished prior to intercalation of the pillaring moieties: the 3-D structure of graphite must be opened with the help of a co-intercalant and this initial hybrid structure must be dispersed in an organic solvent. The role of the co-intercalant is essential because once the graphite planes are pushed apart, guest molecules easily penetrate between the layers with the help of the appropriate solvent [15–17]. Graphite oxide (GO) holds a foremost place in intercalation strategies applied to date because of its well-ordered structure in combination with excellent hydrophilic and swelling properties [18]. The functional oxygen groups (such as hydroxyl, epoxy and carbonyl) give rise to the absorption of polar molecules forming GO-intercalation compounds, however upon reduction the quality of graphene layers is low due to both formation of holes in the hexagonal lattice and the presence of some remaining oxygen-groups.

An alternative is provided by graphite nitrate (GN) whose structure was quite difficult to unravel [19]. The final solution to the puzzle was given by Fuzellier [20] according to whom there are two arrangements of the nitric acid during the intercalation process. The first phase (α crystalline phase) with stoichiometry $C^{+}_{24n}•NO_3$-$5HNO_3$ for the nth stage compound, and interlayer distance of 7.8 Å, corresponds to an arrangement where the triangular planar nitric acid molecules stay perpendicular to the graphite planes. This phase spontaneously converts into a second 'residual' phase (β crystalline phase) with stoichiometry $C^{+}_{24n}•NO_3$-··$2HNO_3$ and an interlayer distance of 6.6 Å, where the molecules lie down between the graphite planes (Fig. 1) [21–23]. The great benefit of using GN as a host matrix for the insertion of suitable robust molecules in the graphite lattice, is the sufficient opening of the graphene layers without any oxidation treatment. Thus, the quality of the graphene flakes after the intercalation remains high and this allows for the development of a new class of hybrid structures with high specific area and defect free lattice.

In this work, we report the successful incorporation of fullerene in GN by a simple intercalation reaction using toluene as solvent. Nitrate molecules/anions play the role of co-intercalant, enabling $C_{60}$ to penetrate between the graphene layers. As a result pillared fullerene-graphene structures are formed upon thermal treatment at relatively low temperatures (below 100 °C). The final hybrid material and the intermediate products were characterized by X-ray diffraction as well as by differential thermal and thermogravimetric (DTA-TGA) analysis, in conjunction with X-ray photoelectron and Raman spectroscopies. The possibility of stabilizing graphite nitrate by intercalation of organic compounds has been tried in the past [24,25], but here we report for the first time the insertion of a robust organic molecule acting as pillar between the graphene layers to create a hybrid structure with good thermal stability.

## 2. Experimental

### 2.1. Materials

High purity graphite powder was purchased from Carbon Bay (grade: SP1, batch no. 04100; lot no. 011705) and toluene (99.99%) from Acros Organics. Nitric acid (fuming, ⩾99.5%, $d = 1.502$ g/cm$^3$), anhydrous acetonitrile (water <10 ppm) and $C_{60}$ (99.5%) were purchased from Sigma–Aldrich. All chemicals were used as received.

### 2.2. Preparation of GN

Graphite powder (4 g) was suspended in 20 ml of fuming nitric acid (⩾99.5%) under vigorous stirring at ambient conditions for 30 min, and the mixture was left to rest for 90 min. Then the top yellow solution (redundant nitric acid) was removed by siphoning, 50 ml of anhydrous acetonitrile was added and the mixture was stirred for another 5 min. The solid phase was separated by filtration through a PTFE membrane with average pore size of 0.45 μm. Finally, the film was washed twice with anhydrous acetonitrile (20 ml each time) and dried under vacuum. The final product (GN) was placed in a brown glass bottle and stored at RT. The weight gain of starting graphite due to adsorption of nitrates was about 30%.

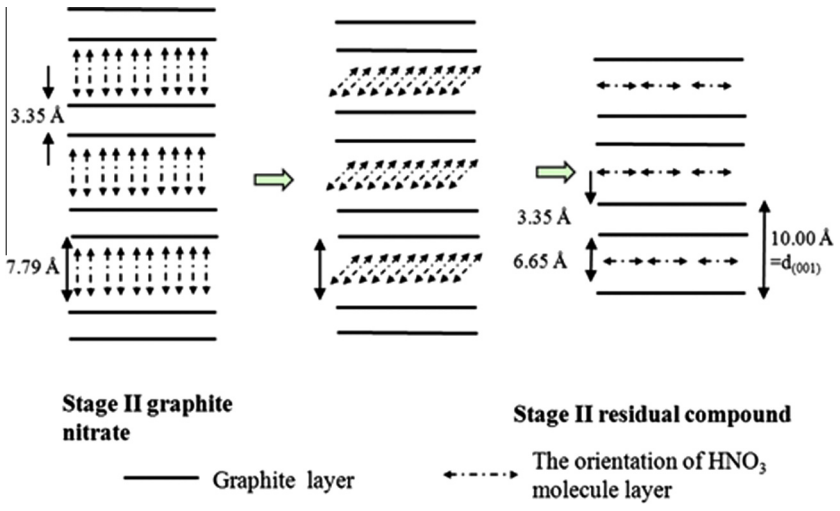


**Fig. 1 – Schematic representation of the stage II graphite intercalation compound formed with $HNO_3$.**

### 2.3. Intercalation of fullerene in GN

In a typical experiment, 10 mg of GN were dispersed in 100 ml of toluene and the mixture was stirred for 5 days at ambient conditions. A solution of $C_{60}$ (10 mg) in toluene (100 ml) was then added dropwise to the graphite nitrate suspension and the mixture was stirred for another 5 days at room temperature. During this progress the initial purple colour of the suspension progressively darkened (after the 3 days) and finally became black indicative of the successful intercalation of $C_{60}$ into the graphite nitrate host material. The mixture was filtered with an Ederol filter (15–65 g/m$^2$, 110 mm), washed three times with toluene and the final powder was collected (sample denoted as GN/$C_{60}$).

### 2.4. Characterization techniques

X-ray diffraction (XRD) data were collected using a Philips PAN anlytical X'Pert MRD diffractometer with a CuK$\alpha$ radiation (40 kV, 40 mA), a 0.25° divergent slit and a 0.125° antiscattering slit. The reflectivity patterns were recorded in the $2\theta$ range from 0.5° to 15° with a 0.02° step and counting time of 10 s per step for the temperature dependent measurements recorded in the range 125–25 °C and a 0.01° step and 15 s of counting time for the room temperature measurements.

Raman spectra were recorded with a Micro–Raman system RM 1000 RENISHAW using a laser excitation line at 532 nm (Nd–YAG) in the range of 1000–2400 cm$^{-1}$. A power of 1 mW was used with 1 μm focusing spot in order to avoid photodecomposition of the samples.

X-ray photoelectron spectroscopy (XPS) data were collected using an SSX-100 (Surface Science Instruments) spectrometer equipped with a monochromatic AlK$\alpha$ X-ray source ($h\nu$ = 1486.6 eV). The photoelectron take off angle was 37° with respect to the surface normal and the energy resolution was set to 1.2 eV. The base pressure in the spectrometer was $3 \times 10^{-10}$ Torr during all measurements. All binding energies were referenced to the C1s core level line [26] of the C–C bond at 285.0 eV and are given ±0.1 eV. Spectral analysis included a Shirley background subtraction and peak deconvolution employing Gaussian–Lorentzian functions in a least squares curve-fitting program (Winspec) developed at the LISE, University of Namur, Belgium. The photoemission peak areas of each element, used to calculate the amount of each species in the probed volume, were normalized by the sensitivity factors of each element, specific to the spectrometer used. The uncertainty in the peak intensity determination is 4% for nitrogen, and 1% for carbon, gold, and oxygen. For the measurements, evaporated polycrystalline gold films supported on mica (grade V-1, TED PELLA), prepared by sublimation of 99.99% gold (Schöne Edelmataal B.V.) were used as substrates. To obtain atomically flat Au(1 1 1) substrates, the sublimation was carried out in a custom built vacuum chamber at a base pressure of $10^{-7}$ Torr onto freshly cleaved mica sheets, which were pre-heated at 650 K for 16 h in order to degas environmental impurities before depositing 150 nm of gold with the mica substrate kept at 650 K. The substrate was cooled down to room temperature over a period of 8 h. After storing under ambient conditions, the substrates were flamed annealed with a hydrogen flame for 1 min in order to eliminate oxygen and carbon impurities from the environmental exposure (immediately before being used for XPS). The samples were prepared by dropcasting a toluene dispersion and dried under vacuum before introduction into the spectrometer.

Thermogravimetric (TGA) and differential thermal (DTA) analysis were performed using a Perkin Elmer Pyris Diamond TG/DTA. Samples of approximately 5 mg were heated in air from 25 to 850 °C, at a rate of 5 °C/min.

## 3. Results and discussion

### 3.1. XRD measurements

XRD patterns of pristine graphite and graphite-nitrate are presented in Fig. 2. The pattern of pure graphite exhibits an intense peak at 26.5° corresponding to a basal spacing of $d_{002}$ = 3.35 Å followed by the weak 1 0 0, 1 0 1 and 0 0 4 reflection peaks at 42.4°, 44.6° and 54.6°. For GN a new 0 0 1 reflection peak appears at 8.8° corresponding to $d_{001}$ = 10.03 Å. The latter corresponds to an intersheet separation of 10.03–3.35 = 6.68 Å where, 3.35 Å is the thickness between two adjacent graphene layers and denotes the formation of a so-called stage II residual compound of GN whose structure is illustrated in Fig. 1 [23]. The stability of this compound depends mainly on temperature; in fact, as demonstrated by the diffraction patterns in Fig. 2, upon heating GN at 100 °C, the nitrate molecules/anions disappear from the graphite galleries and the graphene layers restack forming graphite.

The intercalation of fullerene into the interlayer space of GN was demonstrated by temperature-dependent X-ray diffraction measurements. Fig. 3 displays the XRD patterns of a GN/$C_{60}$ film recorded in a temperature range between 25 and 125 °C. At room temperature, the X-ray diffractogram of GN/$C_{60}$ shows that the main 0 0 1 reflection of GN is superim-

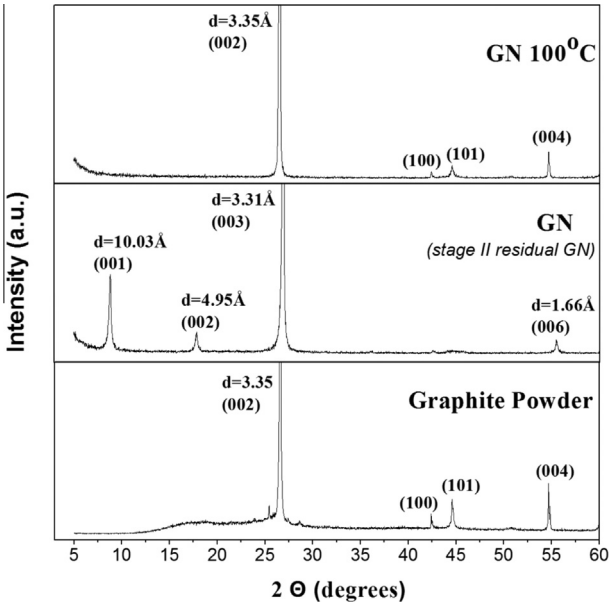


**Fig. 2 – XRD patterns of graphite, graphite nitrate and graphite nitrate after heating at 100 °C.**

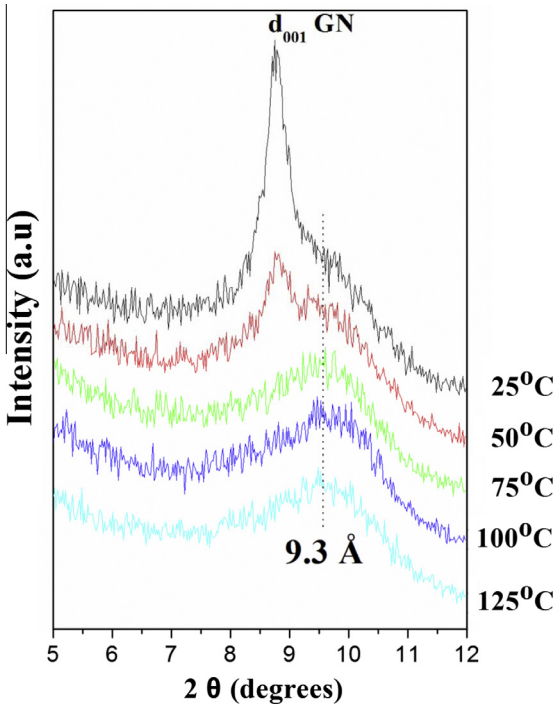


**Fig. 3 – Temperature dependent X-ray diffraction patterns of GN/$C_{60}$.**

posed on a new broader peak centred at ~9.5°. The existence of the 001 peak reveals that the nitrate molecules remain within the graphite galleries (stage II residual compound) while the broad peak is due to insertion of $C_{60}$ molecules between graphene layers, which gives rise to the formation of a new intercalated graphite derivative. As the temperature increases, the 001 peak due to stage II residual GN progressively vanishes. At 75 °C only the broad peak due to $C_{60}$ intercalated between graphene sheets remains and no changes are observed upon further heating, indicating that fullerenes act as robust pillaring molecules between the graphene layers. From the value of the basal $d_{001}$-spacing of 9.3 Å of this compound an intersheet separation of $L$ = 9.3–3.3 = 6.0 Å is deduced, where, the value of 3.3 Å represents the thickness of a graphene sheet. This value is reasonably close to the size of $C_{60}$ (~7 Å) and a similar interlayer spacing has been observed upon intercalation of fulleropyrrolidine derivatives in smectite nanoclays [27]. Employing the Debye–Scherrer equation, the thickness of the coherently diffracting domains or mean crystalline dimension, t, can be calculated: $t = K\lambda/\beta\cos\theta$ [13]. where $K$ is a constant near unity ($K$ = 0.91), $\lambda$ is the wavelength of X-rays ($\lambda$ = 1.5418 Å), $\theta$ is the angular position of the first diffraction peak, and $\beta$ is the broadening of the 001 line diffraction line (calculated as full width at half of the peak height and expressed in radians). Thus the crystalline thickness of the GN/$C_{60}$ hybrids can be estimated as 19.3 Å. As a

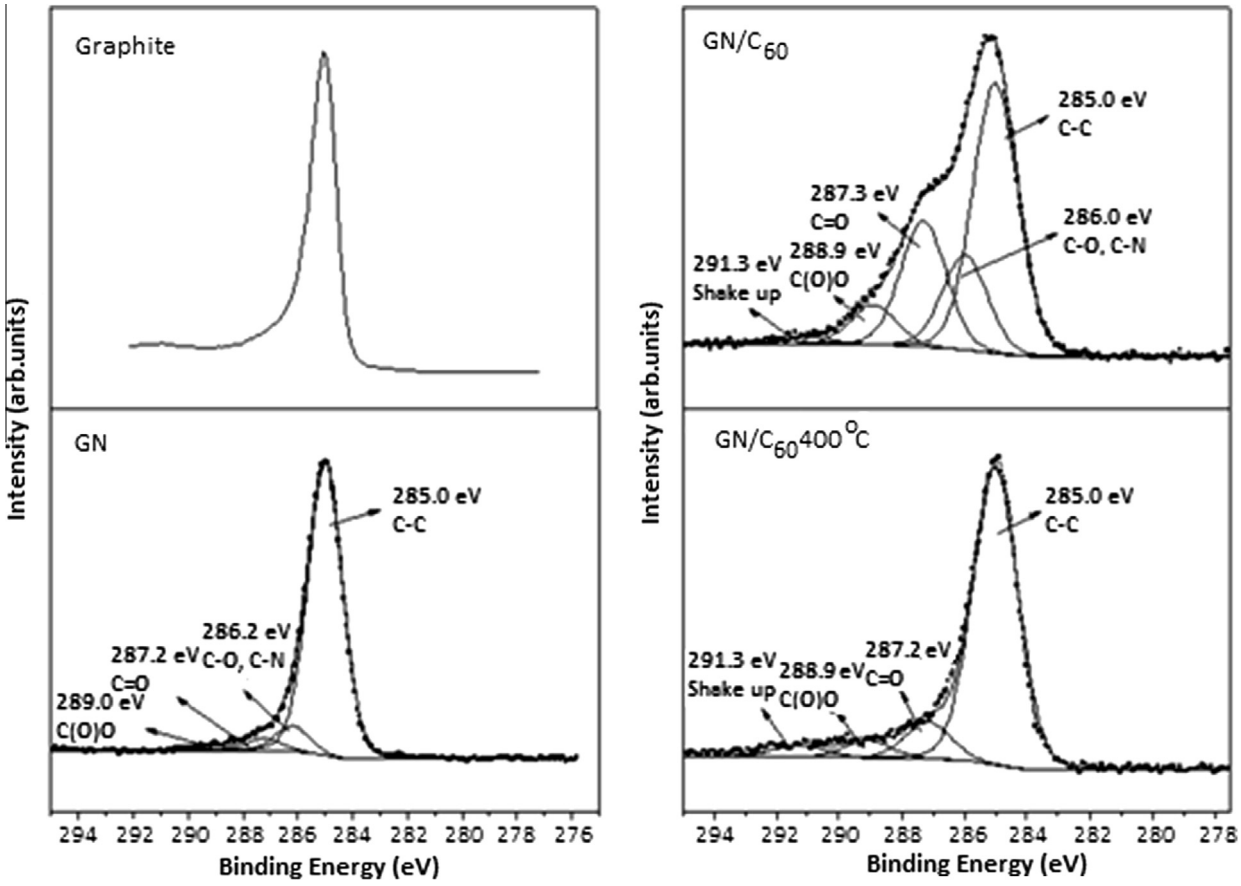


**Fig. 4 – The C1s core level region of the XPS spectra of pristine graphite, graphite nitrate, and graphite nitrate intercalated with $C_{60}$ (GN/$C_{60}$) before and after heating at 400 °C in vacuum.**

**Table 1 – Chemical Compositions of GN and GN/$C_{60}$.**

| GN | | | GN/$C_{60}$ | | |
|---|---|---|---|---|---|
| | Atomic Percentage% | Error % | | Atomic Percentage% | Error % |
| C | 79.6 | 1.6 | C | 72.8 | 1.5 |
| O | 13.8 | 0.8 | O | 22.6 | 1.3 |
| N | 6.6 | 0.8 | N | 4.6 | 0.6 |
| Ratio C/N 12.1 | | | Ratio C/N 15.8 | | |

consequence, the average stacking height of the layers, estimated by the formula $N = t/d$, where $N$ is the number of diffracting layers along the $c$-axis and $d$ is the 001 spacing of one layer (in Å), was found to be equal to two which suggests that an important exfoliation has occurred and that the intercalated hybrid is present as bilayers.

To gain insight into the elemental composition and the chemical state of the elements that make up the pillared compound, XPS spectra of graphite, GN and of the GN/$C_{60}$ hybrid were collected before and after heating at 400 °C (under vacuum) and are presented in Fig. 4. The C1s core level region of the XPS spectrum of natural graphite displays only one narrow peak at a binding energy of 285.0 eV, indicative of the good quality of the starting material. After intercalation of nitric acid, the C1s line of GN exhibits four contributions at 285.0, 286.2, 287.2 and 289.0 eV. The peak at 285.0 eV (C1) originates from the carbon–carbon bonds of the hexagonal lattice, and accounts for 87.5% of the total carbon intensity. The contribution at 286.2 eV (C2) is due to in C–N and C–O bonds (7.8% of the total carbon intensity), while the spectral intensity at 287.2 eV (C3) and 289.0 eV (C4) arises from the carbonyl (3.6%) and carboxyl groups (1.3%), respectively. The data suggest that the synthesis of GN did not significantly affect the graphene lattice since less than 8% of the structure has been functionalized by oxygen and nitrogen containing groups creating defects on the lattice. These findings are in accordance with those obtained by Raman spectroscopy (see below). The C1s core level region of the XPS spectrum of intercalated GN/$C_{60}$ (before heating) reveals the successful intercalation of fullerene whose fingerprint is the shake-up feature centred at 291.3 eV [28,29]. In addition, the same distinct carbon peaks of GN are also observed in the GN/$C_{60}$ hybrid but the relative intensities of these four C1s components are quite different from those of pure GN. In fact, in the GN/$C_{60}$ hybrid, the spectral intensity of the C2–C4 species seems to be increased with respect to that of the C1 species. 16.5% of the total C1s intensity arises from the carbon bound to nitrogen and carbon bound to oxygen (C2), 22.4% comes from the carbonyl groups (C3), while 6.6% stems from the carboxyl groups (C4). This phenomenon could be explained due to the important exfoliation deduced from the XRD data, which causes the photoemission signal of the C2–C4 functionalized carbon groups situated mainly at the edges of the carbon sheets to be less attenuated. In addition, after annealing of the GN/$C_{60}$ material at high temperature (400 °C) under vacuum, a significant reduction of the oxygen/nitrogen containing functional groups is evident from the decreased intensities of the C2–C4 species, attesting to the good quality of the graphene sheets, while the shake-up peak at 291.3 eV remains, confirming the presence of $C_{60}$ molecules between the graphene layers. In detail, after heating the hybrid material 81.7 % of the total C1s intensity corresponds to carbon–carbon bonds of the aromatic ring of graphite, as well the fullerene molecules. Based on the XPS intensities, one also deduces that the oxygen level of the hybrid nanostructure approaches three atomic %; in comparison with other intercalation methods of graphite reported up to now [30], this oxidation level is extremely low.

Since an element's photoemission intensity is directly proportional to its atomic percentage in the probed volume, from the carbon and nitrogen 1s intensities in GN and GN/$C_{60}$ reported in Table 1 one can calculate the intercalation yield. The ratio between the carbon to nitrogen intensities ($I_{C1s}$:$I_{N1s}$) is 12.1 in the pristine GN, and increases to approximately 15.8 after intercalation of $C_{60}$. Assuming that this increase in carbonaceous material is due to the insertion of fullerene into the graphite nitrate matrix ($C^{+}_{48}$•$NO_3$-2$HNO_3$) and hence neglecting the possibility of inserting toluene together with $C_{60}$, we can estimate the intercalation yield as one $C_{60}$ molecule every 155 ± 5 carbon atoms of graphite nitrate.

Fig. 5 presents the Raman spectra of the pristine graphite and GN, as well as of the GN/$C_{60}$ hybrid. The starting graphite material can be classified as defect free and well-ordered since the D band (at around 1350 $cm^{-1}$) is absent [31,32]. After intercalation of nitrate molecules/anions the sharp G peak splits in two peaks at 1580 and 1610 $cm^{-1}$, respectively. The splitting of the G band upon intercalation arises primarily from the symmetry changes since every graphitic layer is now adjacent to an intercalant layer on one side and to a graphene sheet on the other [33,34]. Upon intercalation of $C_{60}$ the intensity ratio of these two bands changes and they broaden considerably: the G band centred at 1580 $cm^{-1}$ dominates the spectrum and the split peak has become so broad that it is visible only as a small shoulder. In addition, in the Raman spectrum of GN/$C_{60}$, a new peak located at 1445 $cm^{-1}$ assigned to the prominent pentagonal pinch mode ($A_g(2)$) of $C_{60}$ reveals the presence of fullerene in the final hybrid material. In fact, this peak is down-shifted 24 $cm^{-1}$ from the $A_g(2)$ mode of fullerite (1469 $cm^{-1}$) [35]. This shifted value is typical for $C_{60}$ adsorbed on surfaces where the molecule interacts only weakly, such as H-terminated Si [36] or CO pre-covered Cu(001) [37], *i.e.*, where neither covalent bonding

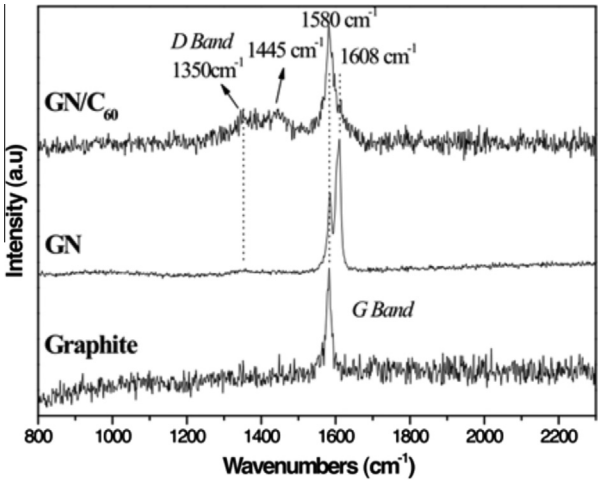


**Fig. 5 – Raman spectra of Graphite, GN and GN/$C_{60}$ at room temperature collected with a laser excitation line at 532 nm.**

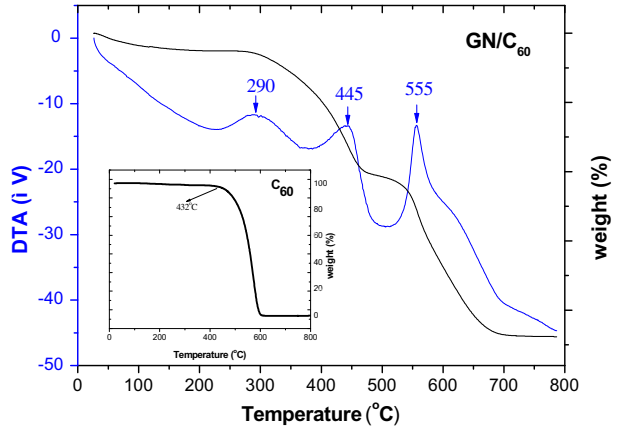


**Fig. 7 – DTA/TGA curves of graphite nitrate intercalated with $C_{60}$ (GN/$C_{60}$). Inset: TGA curve of pure $C_{60}$.**

nor charge transfer occur. One can also see that a small amount of structural disorder is introduced upon intercalation of fullerenes, which translates into the appearance of a small D band (1350 $cm^{-1}$); however, the low relative intensity of the D band with respect to the G band ($I_D/I_G$ ~0.3) is an indication of a fairly well ordered, defect-poor intercalated material [31]. A contribution to the existence of the D band may also come from any remaining toluene which is adsorbed (via π–π stacking) and acts as a donor, transferring electrons to the graphene sheets [38,39].

To investigate the stability of GN and GN/$C_{60}$, thermogravimetric (TGA) analysis was performed. We first compared pure graphite and graphite nitrate before and after heating the sample at 100 °C in air; the results are shown in Fig. 6. Pristine graphite decomposes at temperatures above 680 °C, while GN displays a 23.3% weight loss up to 100 °C; the latter is related to the removal of nitrate molecules/anions, and water molecules from the interlayer space of graphite. Upon further heating GN is found to combust at lower temperatures

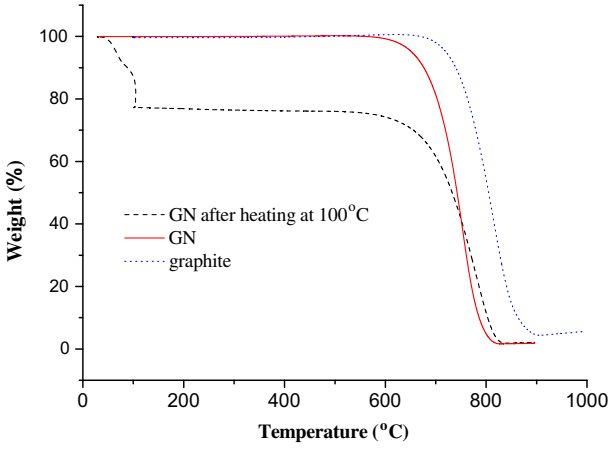


**Fig. 6 – Thermogravimetric analysis curves of pristine graphite, graphite nitrate and graphite nitrate after heating at 100 °C (in air).**

(570 °C) than pristine graphite. In the TG curve of GN collected after heating the sample at 100 °C, the first weight loss step is absent and the combustion of the graphite lattice is taking place at the same temperature as for GN that has not been heated, indicating that nitrate anions were efficiently removed from the graphene galleries without influencing the carbon structure. The lower temperature (with respect to pristine graphite) at which graphitic layers of GN and heated GN start to decompose indicates that opening the interlayer space through intercalation facilitates the access to oxygen even after the intercalant has been evacuated.

After the intercalation of $C_{60}$ into GN, TGA and differential thermal analysis (DTA) were carried out (Fig. 7) to define the characteristics of this hybrid pillared material. GN/$C_{60}$ showed a 6% weight loss up to 150 °C, related, as for GN, to the removal of both nitrate species and intercalated water. Above this temperature, the DTA curve exhibits three exothermic peaks. A 17% weight loss between 230 and 380 °C, with the exothermic peak centred at 290 °C, which is attributed to the removal of oxygen-containing species (see XPS spectra discussed above) from the edges of the graphene sheets and of any toluene co-inserted with $C_{60}$ via adsorption. Toluene is acting as a donor, transferring electrons to graphene [38,39]. The second exothermic peak centred at 445 °C is assigned to the oxidation of intercalated fullerene molecules based on the comparison with the TGA curve of pure fullerene (see inset Fig. 7). From the weight loss curve between 380 and 500 °C, we estimate that about 25 wt% of the total mass corresponds to fullerene molecules incorporated in the hybrid. These results are in accordance with the XPS data where we observe an increase of the C/N ratio of approximately 25%. Finally, for temperatures above 500 °C, the exothermic peak centred at 555 °C originates from the combustion of graphite [40]. This temperature is lower than that of pristine GN (see Fig. 6) and an explanation for this acceleration of the combustion might be that because of the fast temperature rise the graphene layers have no time to re-stack via Van Der Waals interaction [40]. From the TG curve, the total amount of the graphene-based matrix is estimated to be 52 wt% of the overall mass of the hybrid material.

## 4. Conclusions

In conclusion, we demonstrated the successful intercalation of pure fullerene in high quality graphite nitrate derived from reaction of pristine graphite with fuming nitric acid. The nitrate anions play the role of co-intercalant enabling $C_{60}$ molecules (using toluene as solvent) to penetrate between the graphene layers. Heating to temperatures where the nitrate anions diffuse out of the structure yields fullerene-pillared graphene.

The presence of intercalated $C_{60}$ molecules between the graphene sheets is deduced from X-ray diffraction as well as from Raman, and the spectroscopic techniques demonstrate that the quality of the graphene layers is not compromised by the intercalation. A quantification of the interaction yield was derived from thermogravimetric analysis and X-ray photoemission data, yielded that fullerene intercalated in the pillared structure amounts to about 25 wt%.

The present method opens new perspectives for the intercalation of various guest molecules in graphite also because graphite nitrate allows for functionalization processes following the very well established carbon chemistry. Pillaring structures based on graphene (using different type of organic/or inorganic pillars in between the graphene layers) may lead to new types of porous materials suitable as catalysts, catalytic supports or adsorbents for gas storage applications.

## Acknowledgments

This work was performed within "Top Research School" program of the Zernike Institute for Advanced Materials under the Bonus Incentive Scheme (BIS) of the Netherlands' Ministry of Education, Science, and Culture and received additional support from the "Graphene-based Electronics" research program of the 'Stichting voor Fundamenteel Onderzoek der Materie (FOM)', which is financially supported by the 'Nederlandse Organisatie voor Wetenschappelijk Onderzoek (NWO)'. Additionally this research has been co-financed by the European Union (European Social Fund-ESF) and Greek national funds through the Operational Program "Education and Lifelong Learning" of the National Strategic Reference Framework (NSRF) —Research Funding Program: Heracleitus II. Investing in knowledge society through the European Social Fund.

## REFERENCES

[1] Geim AK, Novoselov KS. The rise of graphene. Nat Mater 2007;6(3):183–91.
[2] Meng G, Jung YJ, Cao A, Vajtai R, Ajayan PM. Controlled fabrication of hierarchically branched nanopores, nanotubes, and nanowires. Proc Natl Acad Sci USA 2005;102(20):7074–8.
[3] Zhao XB, Xiao B, Fletcher AJ, Thomas KM. Hydrogen adsorption on functionalized nanoporous activated carbons. J Phys Chem B 2005;109(18):8880–8.
[4] Collins PG, Bradley K, Ishigami M, Zettl A. Extreme oxygen sensitivity of electronic properties of carbon nanotubes. Science 2000;287(5459):1801–4.
[5] Frackowiak E, Beguin F. Carbon materials for the electrochemical storage of energy in capacitors. Carbon 2001;39(6):937–50.
[6] Rodriguez-Reinoso F. The role of carbon materials in heterogeneous catalysis. Carbon 1998;36(3):159–75.
[7] Kayiran SB, Lamari FD, Levesque D. Adsorption properties and structural characterization of activated carbons and nanocarbons. J Phys Chem B 2004;108(39):15211–5.
[8] Steele BCH, Heinzel A. Materials for fuel-cell technologies. Nature 2001;414(6861):345–52.
[9] Davis ME. Ordered porous materials for emerging applications. Nature 2002;417(6891):813–21.
[10] Serp P, Figueiredo JL. Carbon Materials for Catalysis. Hoboken, NJ: John Wiley & Sons, Inc.; 2008.
[11] Stankovich S, Dikin DA, Dommett GHB, Kohlhaas KM, Zimney EJ, Stach EA, et al. Graphene-based composite materials. Nature 2006;442(7100):282–6.
[12] Pinnavaia TJ. Intercalated clay catalysts. Science 1983;220(4595):365–71.
[13] Gournis D, Jankovic L, Maccallini E, Benne D, Rudolf P, Colomer JF, et al. Clay-fulleropyrrolidine nanocomposites. J Am Chem Soc 2006;128(18):6154–63.
[14] Khan AI, O'Hare D. Intercalation chemistry of layered double hydroxides: Recent developments and applications. J Mater Chem 2002;12(11):3191–8.
[15] Liu ZH, Wang ZM, Yang X, Ooi K. Intercalation of organic ammonium ions into layered graphite oxide. Langmuir 2002;18(12):4926–32.
[16] Liu P, Gong K, Xiao P, Xiao M. Preparation and characterization of poly(vinyl acetate)-intercalated graphite oxide nanocomposite. J Mater Chem 2000;10(4):933–5.
[17] Pruvost S, Herold C, Herold A, Lagrange P. Co-intercalation into graphite of lithium and sodium with an alkaline earth metal. Carbon 2004;42(8–9):1825–31.
[18] Bourlinos AB, Gournis D, Petridis D, Szabo T, Szeri A, Dekany I. Graphite oxide: Chemical reduction to graphite and surface modification with primary aliphatic amines and amino acids. Langmuir 2003;19(15):6050–5.
[19] Rüdorff WZ. Crystal structure of acid compounds of graphite. Phys Chem Abt B 1939;45:42–68.
[20] Fuzellier H, Melin J, Herold A. Une nouvelle variete de nitrate de graphite. Mater Sci Eng 1977;31:91–4 (C).
[21] Savoskin MV, Yaroshenko AP, Whyman GE, Mysyk RD. New graphite nitrate derived intercalation compounds of higher thermal stability. J Phys Chem Solids 2006;67(5–6):1127–31.
[22] Moreh R, Shahal O, Kimmel G. Orientation of nitrate molecules in graphite–$HNO_3$ residue compounds. Phys Rev B 1986;33(8):5717–20.
[23] Touzain P. Orientation of nitric acid molecules in graphite nitrate. Synth Met 1979;1(1):3–11.
[24] Inagaki M. Applications of graphite intercalation compounds. J Mater Res 1989;4(6):1560–8.
[25] Savos'kin MV, Yaroshenko AP, Mysyk RD, Vaiman GE, Vovchenko LL, Popov AF. Stabilization of graphite nitrate by intercalation of organic compounds. Theor Exp Chem 2004;40(2):92–7.
[26] Lotya M, Hernandez Y, King PJ, Smith RJ, Nicolosi V, Karlsson LS, et al. Liquid phase production of graphene by exfoliation of graphite in surfactant/water solutions. J Am Chem Soc 2009;131(10):3611–20.
[27] Gournis D, Georgakilas V, Karakassides MA, Bakas T, Kordatos K, Prato M, et al. Incorporation of fullerene derivatives into smectite clays: A new family of organic–inorganic nanocomposites. J Am Chem Soc 2004;126(27):8561–8.
[28] Leiro JA, Heinonen MH, Laiho T, Batirev IG. Core-level XPS spectra of fullerene, highly oriented pyrolitic graphite, and glassy carbon. J Electron Spectrosc Relat Phenom 2003;128(2–3):205–13.

[29] Kumar A, Singh F, Govind, Shivaprasad SM, Avasthi DK, Pivin JC. X-ray photoelectron and X-ray auger electron spectroscopy studies of heavy ion irradiated $C_{60}$ films. Appl Surf Sci 2008;254(22):7280–4.
[30] Viculis LM, Mack JJ, Mayer OM, Hahn HT, Kaner RB. Intercalation and exfoliation routes to graphite nanoplatelets. J Mater Chem 2005;15(9):974–8.
[31] Nemanich RJ, Solin SA. First- and second-order Raman scattering from finite-size crystals of graphite. Phys Rev B 1979;20(2):392–401.
[32] Katagiri G, Ishida H, Ishitani A. Raman spectra of graphite edge planes. Carbon 1988;26(4):565–71.
[33] Afanasov IM, Shornikova ON, Kirilenko DA, Vlasov II, Zhang L, Verbeeck J, et al. Graphite structural transformations during intercalation by $HNO_3$ and exfoliation. Carbon 2010;48(6):1862–5.
[34] Dresselhaus MS, Dresselhaus G. Intercalation compounds of graphite. Adv Phys 2002;51(1):1–186.
[35] Haddon RC, Hebard AF, Rosseinsky MJ, Murphy DW, Duclos SJ, Lyons KB, et al. Conducting films of $C_{60}$ and $C_{70}$ by alkali-metal doping. Nature 1991;350(6316):320–2.
[36] Dumas P, Gruyters M, Rudolf P, He Y, Yu LM, Gensterblum G, et al. Vibrational study of $C_{60}$ overlayers on H/Si(1 1 1)-$(1 \times 1)$. Surf Sci 1996;368(1–3):330–6.
[37] Rudolf P, Raval R, Dumas P, Williams GP. Vibrational dynamics of fullerene molecules adsorbed on metal surfaces studied with synchrotron infrared radiation. Appl Phys A 2002;75(1):147–53.
[38] Kaverzin AA, Strawbridge SM, Price AS, Withers F, Savchenko AK, Horsell DW. Electrochemical doping of graphene with toluene. Carbon 2011;49(12):3829–34.
[39] Boukhvalov DW. Tuneable molecular doping of corrugated graphene. Surf Sci 2010;604(23–24):2190–3.
[40] Pang LSK, Saxby JD, Chatfield SP. Thermogravimetric analysis of carbon nanotubes and nanoparticles. J Phys Chem 1993;97(27):6941–2.